International Journal of Engineering Trends and Technology
ISSN: 2231 – 5381 / https://doi.org/10.14445/22315381/IJETT-V70I7P207
Volume 70 Issue 7, 60-67, July 2022

Original Article

Improved Classification of Intact Ripe Mango Sweetness using Fusion Deep Learning and Enhanced Near-Infrared Spectroscopy

Sumitra Nuanmeesri[1], Lap Poomhiran[2]

[1]*Faculty of Science and Technology, Suan Sunandha Rajabhat University, Bangkok, Thailand*
[2] *Faculty of Information Technology and Digital Innovation, King Mongkut's University of Technology North Bangkok, Bangkok, Thailand*

[1]sumitra.nu@ssru.ac.th

Received: 14 May 2022 Revised: 27 June 2022 Accepted: 04 July 2022 Published: 18 July 2022

Abstract *- This research aims to develop models for classifying the sweetness of intact ripe mangoes using image-based deep learning fused with near-infrared spectral data. Each mango was measured for near-infrared spectral data at all 12 locations distributed across the fruit. These spectral data were enhanced by Baseline Linear Correction, Multiplicative Scatter Correction, Standard Normal Variate, and mixed methods. Next, the mango images are processed using the GrabCut method to eliminate background information and then adjusted with the Adaptive Mean-C Thresholding method. Finally, the mango fruit image was processed, and the enhanced spectral data were taken through feature extraction using a Convolutional Neural Network-based early fusion technique. The results showed that the model using the enhanced spectral data that applied the Multiplicative Scatter Correction combined with the Standard Normal Variate method provided the highest model efficiency. The training accuracy was 99.66%, and this model's validation accuracy was 94.20%. Therefore, enhanced near-infrared spectroscopy, combined with image processing and model development deep learning-based, can improve the classification of the sweetness of ripe mangoes.*

Keywords *- Classification, Deep Learning, Mango Sweetness, Near-Infrared, Neural Network.*

1. Introduction

Mango (*Mangifera indica* L.) is a popular tropical fruit worldwide that can be eaten raw and ripe. Over one thousand varieties of mangoes are cultivated worldwide, and over one hundred seventy-two varieties are cultivated in Thailand [1]. It contains many nutrients, such as vitamins A, C, E, and B6 [2]. It is also rich in potassium, folate, and beta-carotene [3], an antioxidant. Moreover, mango contains high dietary fiber [2] that helps lose weight [3]. Besides, mangoes also contain fructose, glucose, and sucrose. The amount of sucrose is higher than other sugars in mango. Over several days, the mango will begin to ripen and increase its sugar content [4]. However, eating ripe or overripe mangoes will cause the body to get more sugar than necessary. The excess amount of sugar accumulated in the body can harm the functioning of the body and can lead to diabetes. In this case, it usually occurs quickly in older people or those at risk of developing diabetes. Therefore, avoiding ripe or overripe mangoes is another approach for these at-risk individuals.

The ripeness of mangoes requires expertise in observing the mangoes in many aspects, including smelling, plumpness, skin color, and wrinkles on the peel. Sometimes the plumpness or shape of the fruit is not a sure measure of the mango sweetness that has more sugar. Because some mango fruits may not have an extensive size, they are maturing or fully ripe. In addition, ripened mangoes are less sweet than those that are naturally ripe mangoes. Generally, each ripe mango variety and each fruit have a different amount of sugar. Thus, it may be more challenging to predict the sweetness or sugar content of ripe mangoes by observation.

A wide variety of research has classified the quality of mangos by using near-infrared (NIR) spectroscopy [2], [5]–[9] with wavelengths in the 1,000 to 2,500 nanometers (nm). This method will not damage the fruit. Raw NIR spectroscopy data may be classified directly with the Random Forest classifier [9] or other methods. For most research, raw NIR spectral data is obtained through noise or scatter methods [7], such as Standard Normal Variate (SNV), Multiplicative Scatter Correction (MSC), and Unit Vector Normalization (UVN) [8]. This approach makes the model more efficient in its classification when applied to the classifier. Some studies take NIR spectral data through a deep learning process using applications to classify coffee [10] and peach cultivars [11]. In addition, mango images are

subjected to image processing to classify sweetness [12], ripeness [13], and the quality of mangoes [14]. However, from the present research, most mangoes are classified by one of the abovementioned methods. There is significantly less research on how these techniques can be applied together. Therefore, this research aims to apply various techniques together to classify the sweetness of mangoes without damaging the fruit based on Convolutional Neural Network (CNN) with image processing fused with the enhanced NIR spectral data

2. Methodology

Improving the efficiency of classifying the sweetness of ripe mangos by methods that intact the fruit relies mainly on image processing and the spectrum data in the NIR region. The mango fruit data was then taken through a deep learning technique to predict how ripe the mango was and how much range of sugar it contained. The method of this work was described as the following processes.

2.1. Data Collection

This research selected popular ripe mangos that Thai people like to eat and can easily be bought in the fresh market. Thus, these favorite ripe mangoes include Okrong, Okrong Thong, Namdokmai, and Namdokmai Si-Thong. Consequently, eight hundred eighty mangoes were collected that were mixed from all four varieties of mangoes mentioned above. These mangoes consisted of one hundred thirteen unripe, four hundred eighty-nine ripe, and two hundred seventy-eight overripe, as shown in Table 1.

Table 1. Amount of collected mangoes

Mango varieties	Number of mango fruits			Total
	Unripe	Ripe	Overripe	
Okrong	27	115	69	211
Okrong Thong	32	127	64	223
Namdokmai	26	129	70	225
Namdokmai Si-Thong	28	118	75	221
Summary	**113**	**489**	**278**	**880**

All mangoes collected will be recorded for each fruit specification in three steps.

2.1.1. Mango images

Take a photo of the mango fruits in the top view on both the left and right sides of each mango. Thus, there will be one thousand seven hundred sixty images of mango fruit. All images were labeled with the running numbering of the sample.

2.1.2. NIR spectral data

All mangoes were scanned with a NIR sensing device (PSD-FTNIR i16) in wavelengths between 1,000 nm and 2,500 nm. The resolution windows were set to 0.02 nm with 4x optical gain. Each mango side was scanned at six different locations: top-left, top-right, middle-left, middle-right, bottom-left, and bottom-right positions, as shown in Fig. 1. The absorbance spectrum output of NIR spectral data for both left and right sides of mango were collected in comma-separated values (CSV) file formatted**.**

2.1.3. Measuring sweetness

This process requires cutting or segmenting mango to measure the sweetness. One mango can be unevenly sweet, with the top part being sweeter than the bottom. Therefore, in this research, mango pulp was cut on both sides of the fruit and divided into six pieces: top-left, top-right, middle-left, middle-right, bottom-left, and bottom-right sections. Next, the authors applied the refractometer with automatic temperature compensation (ATC) that has a resolution between 0 and 32% Brix to measure the sweetness of all twelve pieces of mango pulp, as shown in Fig. 2. Last, all sweetness values for each side of the mango were average and then recorded to the previous CSV file.

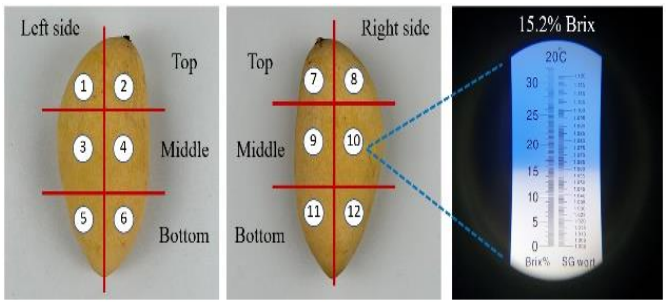

Fig. 2 Mango pulp segmentation and sweetness measuring

This work categorized the mango sweetness into ten levels for classification, as shown in Table 2.

Table 2. The mango sweetness levels

Levels	Sweetness (%Brix)
A	<= 8.0
B	8.1 – 10.0
C	10.1 – 12.0
D	12.1 – 14.0
E	14.1 – 16.0
F	16.1 – 18.0
G	18.1 – 20.0
H	20.1 – 22.0
I	22.1 – 24.0
J	> 24.0

2.2. Image Preprocessing

All images of mango fruit are processed to make the texture features on the mango peel surface more prominent. This research consists of 3 steps of image processing as follows.

2.2.1. Image cropping and resizing

All images are cropped to a square shape and resized to 224x224 pixels suitable for VGG16 [15] based deep learning processing.

2.2.2. Remove background information

The GrabCut [16] algorithm was applied to remove background data leaving only the mango image. The GrabCut algorithm is based on the graph technique by applying the border matting and foreground estimation. The example of image output is shown in Fig. 3. These mango images were kept to the first image dataset.

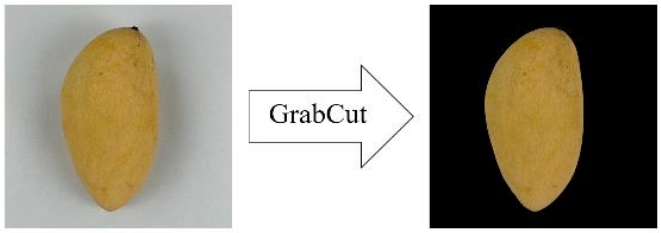

Fig. 3 Example of the mango image output by GrabCut

2.2.3. Image Thresholding

The image of the mango with the background removed is enhanced by image thresholding processing. Start by blurring the image with the median blur method. Then adjust thresholding using Adaptive Mean-C Thresholding where the constant value C was 3. Finally, use binary thresholding to adjust the image to reverse the image between white and black. The example of the final image output is shown in Fig. 4. These mango images were kept to the second image dataset

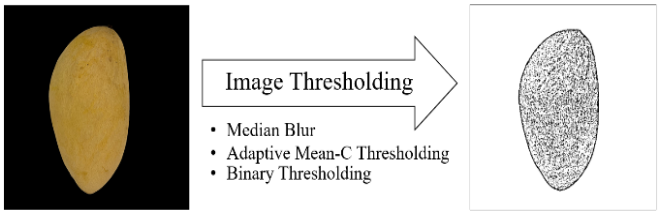

Fig. 4 Example of the mango image output by GrabCut

Therefore, there are two mango image datasets, including the mango image without background information and the mango image in which image thresholding is processed.

2.3. NIR Spectral Data Enhancement

All raw NIR spectral data were transformed by applying the BLC, MSC, and SNV techniques.

2.3.1. BLC

The BLC method is used to eliminate the noise of spectral data [17] as in (1) [18].

$$y_i = ax_i + b \ (i \in W) \tag{1}$$

Where:

y_i represents the fitting value of spectral data of wavelength *i*;

a represents the first-order regression coefficients;

x_i represents the spectral data of wavelength *i*;

b represents the first-order regression coefficients;

W represents the set of wavelengths.

2.3.2. MSC

The MSC method compensates for additional and multiplicative effects that physical effects may cause in the spectral data [19] by eliminating irrelevant scattering [20] as in (2) [21].

$$Z(v) = a + b \cdot Z_r(v) + e \tag{2}$$

Where:

Z(v) represents the model according to the reference spectrum;

$Z_r(v)$ represents the reference spectrum data;

a represents the additive baseline factor;

b represents the multiplicative factor;

e represents the remaining variable that was not modeled.

2.3.3. SNV

This method does not require the model. It is a fast implementation for scatter correction [22]. The SNV can remove the slope variation of the raw spectral data and correct the scattered light effectively [20] as in (3) [23].

$$x_{i,j}(snv) = \frac{(x_{i,j} - \bar{x}_i)}{\sqrt{\frac{\sum_{j=1}^{p}(x_{i,j} - \bar{x}_i)^2}{p-1}}} \tag{3}$$

Where:

$x_{i,j}(snv)$ represents the component of the transformed spectral data;

$x_{i,j}$ represents the correspondence of the primary component of the spectral data *i* for the variable *j*;

$\bar{x}_i$ represents the average of spectral data *i*;

p represents the number of wavelengths in the spectral data.

2.3.4. MSC+BLC

The BLC and MSC were based on the linear correction. This work applied the BLC then MSC method for raw spectral data of mango.

2.3.5. MSC+SNV

This method is the combination of MSC and SNV. First, the SNV is used to eliminate the slope variation then the MSC is used to eliminate the irrelevant scatter.

2.4. Deep Learning Modeling

The architecture of the models for classifying the mango sweetness is based on the VGG16 and 1D CNN architecture combined with the early fusion technique.

2.4.1. VGG16 architecture

This architecture has five blocks of convolution layers of 3x3 kernel size with one stride and Rectified Linear Unit (ReLU) activation function. The filters were incremented

from 64, 128, 256, and 512 for the convolution blocks. In total, there are thirteen convolution layers. The 2x2 max-pooling was applied with two strides at the end of each convolution block. Last, there is one flatten layer to optimize the feature to 1-dimensional data of mango image datasets.

2.4.2. 1D CNN architecture

All six NIR spectral data were set as 1-dimensional input data for 1D convolution layers. This architecture includes four convolution layers with a 20 filter size. The number of filters was incremented from 32, 64, 128, and 256, respectively. The ReLU activation function was applied for all convolution layers. There are four max-pooling which have the filter sizes were 2, 5, 5, and 5, respectively. The dropout was set to 0.1 at the end of the 1D CNN architecture, then flattened.

2.4.3. Fusion and classifying

All flattened output from VGG16 and 1D CNN architecture were fused and then classified by applying the two dense (4,096), two dropouts (0.1), and softmax activation function for the last layers. The proposed model architecture is shown in Fig. 5.

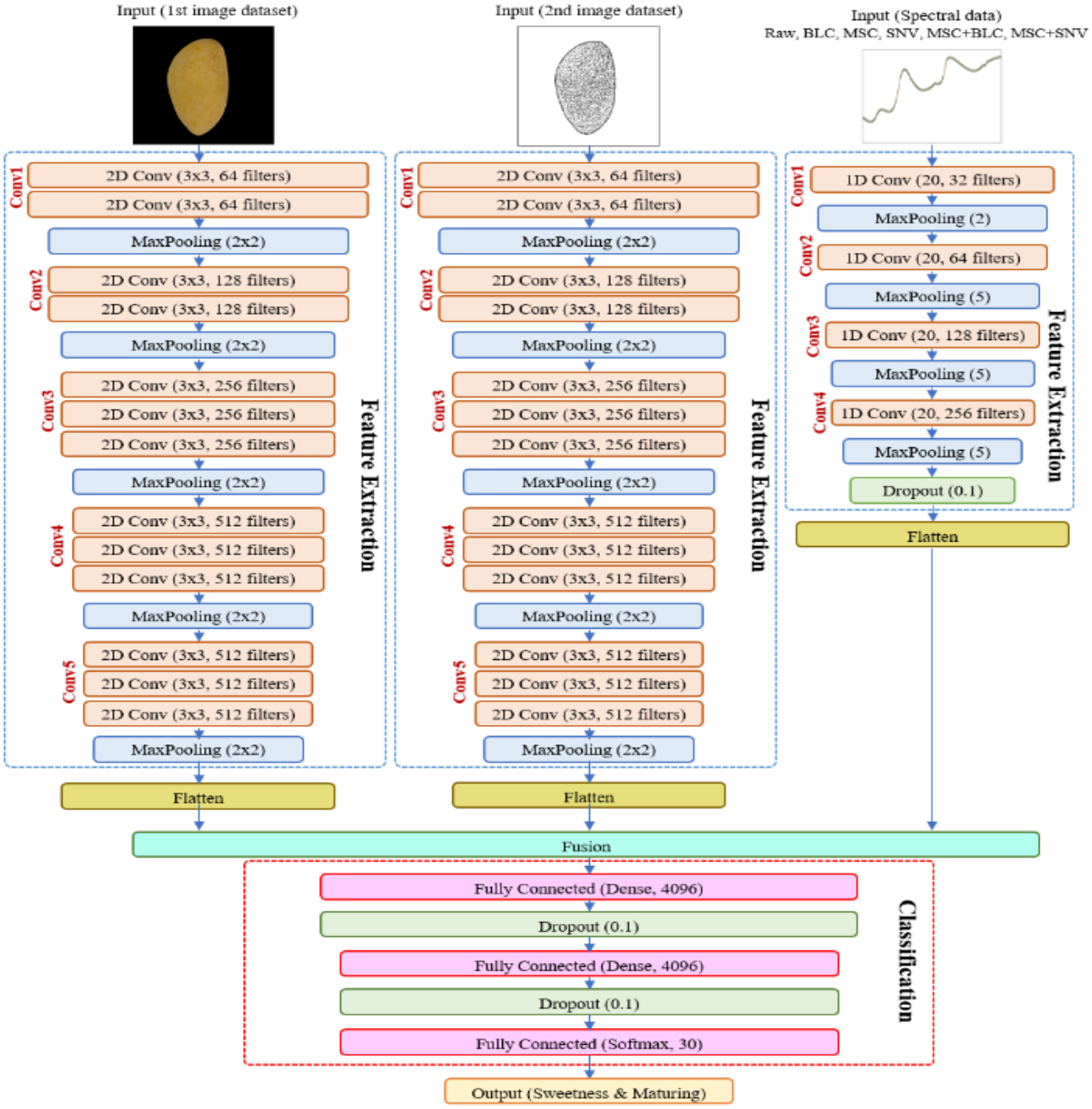

Fig. 5 The proposed model architecture

According to Fig. 5, the two datasets, including the mango image without background information and the thresholded mango image, were used to train and test with the designed VGG16 architecture for image feature extraction. Only the six NIR spectral data were applied for the 1D CNN architecture. Each dataset was split into 80% for the training set and 20% for the test set. During the model's training for 300 epochs, the early stopping was applied to monitor the accuracy with the patient was 7. This early stopping was used to eliminate the model overfitting. Moreover, the learning rate was 0.01, and the batch size was 16.

2.5. The Model Efficiency Evaluation

After all six models were trained and tested, each model evaluated the efficacy by applying the accuracy, sensitivity, precision, specificity, and F-measure by formula (4), (5), (6), (7), and (8) [24]–[26], respectively.

$$Accuracy = \frac{TP+TN}{TP+TN+FP+FN} \quad (4)$$

$$Sensitiviy = \frac{TP}{TP+FN} \quad (5)$$

$$Precision = \frac{TP}{TP+FP} \quad (6)$$

$$Specificity = \frac{TN}{TN+FP} \quad (7)$$

$$F-measure = \frac{2\times Precision\times Sensitivity}{Precision+Sensitivity} \quad (8)$$

Where:

TP represents the output class is true while the actual class is true;

TN represents the output class is false while the actual class is false;

FP represents the output class is true while the actual class is false;

FN represents the output class is false while the actual class is true.

Moreover, the models were validated using the 10-Fold Cross-Validation to evaluate the efficiency of the model's validation. Therefore, a model framework of all processes in this work is shown in Fig. 6.

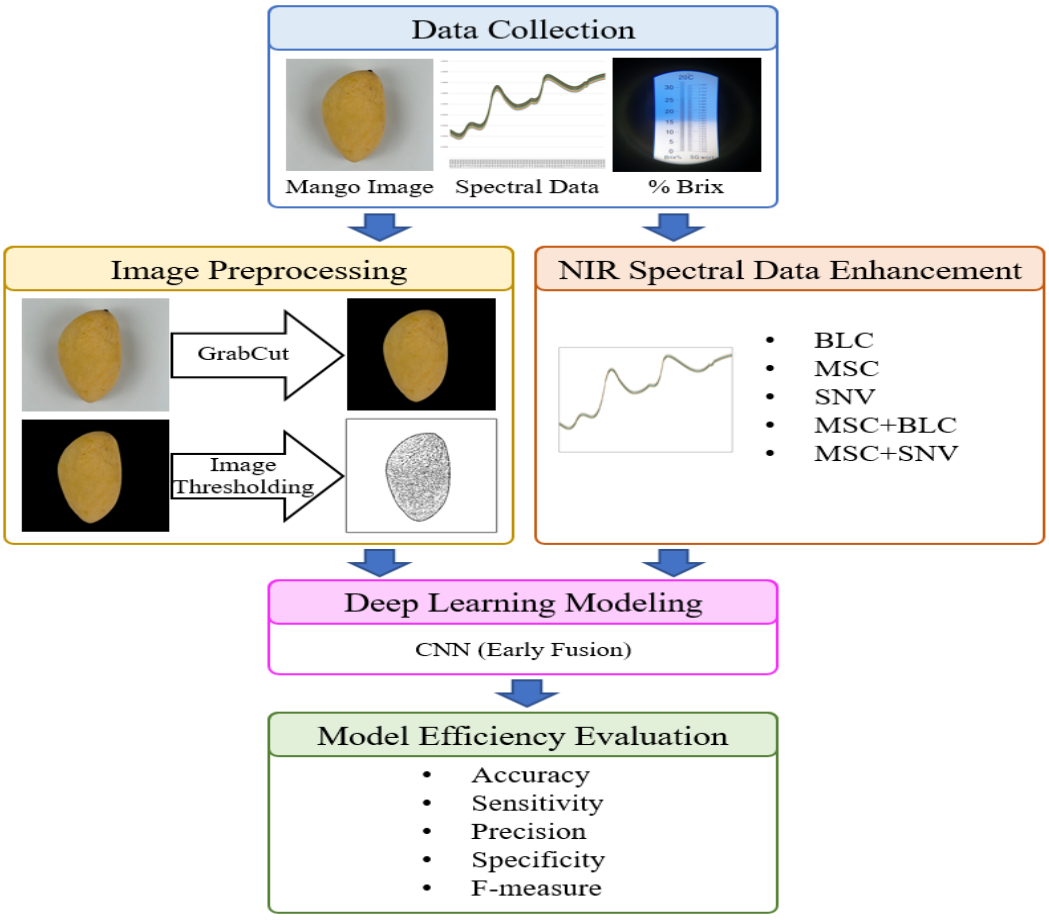

Fig. 6 The research model framework

3. Result

3.1. The Result of Efficiency of Model's Traning

After the six models were trained with six datasets, including raw spectral data, BLC, MSC, SNV, MSC+BLC, and MSC+SNV, it was found that the model which is developed by using the MSC+SNV dataset has the highest efficiency. This model gave the accuracy (Acc) was 99.66%, the sensitivity (Sens) was 99.33%, the precision (Prec) was 99.83%, the specificity (Spec) was 99.65%, and the F-measure was 99.75%. The most efficient models for the remaining models with the efficiency of model training are MSC+BLC, SNV, MSC, BLC, and raw spectral data, respectively. The model training accuracy of these models was 99.20%, 98.75%, 98.07%, 97.39%, and 96.93%, respectively. The efficiency of the model's training of all the six models is shown in Table 3.

Table 3. The efficiency of the model's training

Models	Acc	Sens	Prec	Spec	F-measure
Raw	96.93	97.48	97.97	95.79	97.73
BLC	97.39	97.82	98.31	96.49	98.06
MSC	98.07	98.49	98.65	97.19	98.57
SNV	98.75	98.99	99.16	98.25	99.07
MSC+BLC	99.20	99.33	99.49	98.95	99.41
MSC+SNV	99.66	99.66	99.83	99.65	99.75

3.1.1. The Result of Efficiency of Model's Validation

The developed model with the MSC+SNV dataset has generated the highest efficacy compared to the other models in this work. The MSC+SNV model's efficiency includes the accuracy of 94.20%, the sensitivity of 94.97%, the precision of 96.42%, the specificity of 92.61%, and the F-measure of 95.69%. The model with the second model's validation efficiency is the MSC+BLC model. It gave a validation accuracy was 93.52%. Next, the SNV model, MSC model, BLC model, and raw spectral data model with the validation accuracy were 92.61%, 92.16%, 91.70%, and 90.45%, respectively.

In addition, the result of the efficiency of the model's validation, such as the accuracy, sensitivity, precision, specificity, and F-measure values, was shown in Table 4.

Table 4. The efficiency of the model's validation

Models	Acc	Sens	Prec	Spec	F-measure
Raw	90.45	91.04	94.82	89.17	92.89
BLC	91.70	92.36	95.37	90.29	93.84
MSC	92.16	92.85	95.55	90.68	94.18
SNV	92.61	93.33	95.73	91.07	94.51
MSC+BLC	93.52	94.15	96.24	92.20	95.18
MSC+SNV	94.20	94.97	96.42	92.61	95.69

All the model efficiency results were compared, as shown in Figure 7.

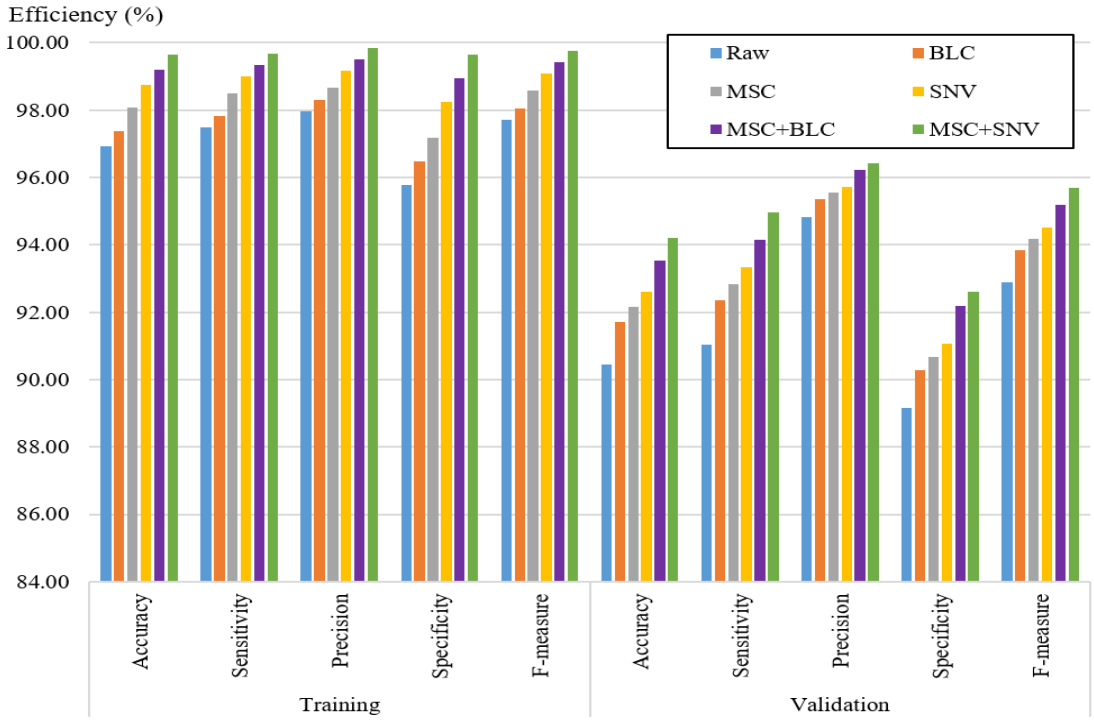

Fig. 7 The comparison of the model efficiency results

4. Conclusion

Mangoes are nutritious and versatile fruit when eaten during the proper ripening period. However, the amount of sugar found will vary according to the ripening period of the mango fruit. This research used data from 880 mangoes, consisting of mango species, Okrong, Okrong Thong, Namdokmai, and Namdokmai Si-Thong. These mangoes were photographed on both the left and right sides of the mango fruit. Then take all the mango fruit images by cutting out the background information using the GrabCut technique. Next, the mango images without background information were processed using Adaptive Mean-C Thresholding. This method makes essential features on the mango peel clearer, such as rough, wrinkled, or bruised skin. Then, each mango fruit was measured with the near-infrared spectral data of mango fruits at different locations of all 12 positions. The near-infrared spectral data of each mango were enhanced by BLC, MSC, SNV, MSC+BLC, and MSC+SNV methods. In addition, the sweetness of each mango was also measured by a refractometer with ATC. The resulting sweetness value was used to compare the accuracy of sugar sweetness classification with the developed models.

In this research, the sweetness of mango fruit was classified from the dataset using a deep learning approach with Convolutional Neural Networks based on the VGG16 architecture for 2-dimensional and 1-dimensional convolution layers. Each output data from CNN architecture was fusion and then classified as mango sweetness. A total of six models were developed using a mango fruit image dataset without background data, an adaptive Mean-C Thresholding mango fruit image, and raw or enhanced spectral data. The result shows that the developed model using the Multiplicative Scatter Correction and Standard Normal Variate techniques is the highest efficiency for classifying the mango sweetness. Furthermore, the training accuracy of this model was 99.66%, and the validation accuracy was 94.20%. Therefore, the model developed in this way can be used in further development as an application for classifying sweetness levels in Mango, Okrong, Okrong Thong, Namdokmai, and Namdokmai Si-Thong.

In this research, mainly four varieties of mango were covered. However, there are hundreds of cultivars of mangoes. Therefore, if the proposed method is to be applied in conjunction with other mango cultivars, it can be done by applying the other mango fruit images and spectral data of the desired mango varieties for further training. This resulting model can be used as transfer learning to reduce the process and increase classification efficiency.

Acknowledgment

The authors would like to thank the Institute for Research and Development, Suan Sunandha Rajabhat University, and the Faculty of Information Technology and Digital Innovation, King Mongkut's University of Technology North Bangkok, for supporting and giving work opportunities.

References

[1] P. Pinsirodom, R. Taprap, and T. Parinyapatthanaboot, "Antioxidant Activity and Phenolic Acid Composition in Different Parts of Selected Cultivars of Mangoes in Thailand," *International Food Research Journal,* vol. 25, no. 4, pp. 1435-1443, 2018.

[2] Kusumiyat, A.A. Munawar, and D. Suhandy, "Fast and Contactless Assessment of Intact Mango Fruit Quality Attributes Using Near Infrared Spectroscopy (NIRS)," *IOP Conference Series: Earth and Environmental Science,* Banda Aceh, Indonesia: IOPScience, vol. 644, pp. 012028, 2021.

[3] Y. Papanikolaou and V.L. Fulgoni III, "Mango Consumption is Associated with Improved Nutrient Intakes, Diet Quality, and Weight-Related Health Outcomes, Nutrients," vol. 14, no. 1, pp. 59, 2022.

[4] Md.K. Islam, M.Z.H. Khan, M.A.R. Sarkar, N. Absar, and S.K. Sarkar, "Changes in Acidity, TSS, and Sugar Content at Different Storage Periods of the Postharvest Mango (Mangifera Indica L.) Influenced by Bavistin DF," *International Journal of Food Science*, vol. 2013, pp. 939385, 2013.

[5] A.A. Munawar, Kusumiyati, and D. Wahyuni, "Near Infrared Spectroscopic Data for Rapid and Simultaneous Prediction of Quality Attributes in Intact Mango Fruits," *Data in Brief,* vol. 27, pp. 104789, 2019.

[6] A. Raghavendra, D.S. Guru, and M.K. Rao, "Mango Internal Defect Detection Based on Optimal Wavelength Selection Method Using NIR Spectroscopy," *Artificial Intelligence in Agriculture*, vol. 5, pp. 43-51, 2021.

[7] A.A. Munawar, D.v. Hörsten, D. Mörlein, E. Pawelzik, and J.K. Wegener, "Rapid and Non-Destructive Prediction of Mango Sweetness and Acidity Using Near Infrared Spectroscopy," in Proc. *Mass Data Management in the Agricultural and Food Industry - Collection - Processing - Use,* pp. 219-222, 2013.

[8] M.S. Amirul, R. Endut, C.B.M. Rashidi, S.A. Aljunid, N. Ali, M.H. Laili, A.R. Laili, and M.N.M. Ismail, "Estimation of Harumanis (Mangifera indica L.) sweetness using Near-Infrared (NIR) Spectroscopy," *IOP Conference Series: Materials Science and Engineering*, vol. 767, no. 1, pp. 012070, 2020.

[9] C.-N. Nguyen, Q.-T. Phan, N.-T. Tran, M. Fukuzawa, P.-L. Nguyen, and C.N. Nguyen, "Precise Sweetness Grading of Mangoes (Mangifera Indica L.) Based on Random Forest Technique with Low-Cost Multispectral Sensors," *IEEE Access*, vol. 8, pp. 212371-212382, 2020.

[10] Y.T. Chang, M.C. Hsueh, S.P. Hung, J.M. Lu, J.H. Peng, and S.F. Chen, "Prediction of Specialty Coffee Flavors Based on Near-Infrared Spectra Using Machine and Deep-Learning Methods," *Journal of the Science of Food and Agriculture*, vol. 101, pp. 4705-4714, 2021.

[11] D. Rong, H. Wang, Y. Ying, Z. Zhang, and Y. Zhang, "Peach Variety Detection Using VIS-NIR Spectroscopy and Deep Learning," *Computers and Electronics in Agriculture*, vol. 175, pp. 105553, 2020.
[12] S.K. Bejo and S. Kamaruddin, "Determination of Chokanan Mango Sweetness (Mangifera Indica) Using Non-Destructive Image Processing Technique," *Australian Journal of Crop Science*, vol. 8, no. 4, pp. 457-480, 2014.
[13] M.F. Mavi, Z. Husin, B.A., Y.M. Yacob, R.S.M. Farook, W.K. Tan, Mango ripeness classification system using hybrid technique, Indonesian Journal of Electrical Engineering and Computer Science. 14(2) (2019) 859-868.
[14] K. Ratprakhon, W.C. Neubauer, K. Riehn, J. Fritsche, and S. Rohn, Developing an Automatic Color Determination Procedure for the Quality Assessment of Mangos (Mangifera Indica) Using a CCD Camera and Color Standards," *Foods*, vol. 9, 2020.
[15] K. Simonyan and A. Zisserman, "Very Deep Convolutional Networks for Large-Scale Image Recongnition," arXiv preprint, arXiv:1409.1556, 2015.
[16] G. Rother, V. Kolmogorov, and A. Blake, "GrabCut: Interactive Foreground Extraction Using Iterated Graph Cuts," in Proc. *ACM Transactions on Graphics*, vol. 23, no. 3, pp. 309-314, 2004.
[17] R. Hayati, A.A. Munawar, and F. Fachruddin, "Enhanced Near Infrared Spectral Data to Improve Prediction Accuracy in Determining Quality Parameters of Intact Mango," *Data in Brief*, vol. 30, pp. 105571, 2020.
[18] F. Zhang, X. Tang, A. Tong, B. Wang, and J. Wang, "An Automatic Baseline Correction Method Based on the Penalized Least Squares Method," *Sensors*, vol. 20, pp.2015, 2020.
[19] A.A. Munawar, Y. Yunus, Devianti, and P. Satriyo, "Calibration Models Database of Near Infrared Spectroscopy to Predict Agricultural Soil Fertility Properties," *Data in Brief*, vol. 30, pp. 105469, 2020.
[20] G. Ren, Y. Sun, M. Li, J. Ning, and Z. Zhang, "Cognitive Spectroscopy for Evaluating Chinese Black Tea Grades (Camellia Sinensis): Near-Infrared Spectroscopy and Evolutionary Algorithms," *Journal of the Science of Food and Agriculture*, vol. 100, pp. 3950-3959, 2020.
[21] H.U. Rehman et al., "Preclassification of broadband and sparse infrared data by multiplicative signal correction approach, Molecules," vol. 27, pp. 2298, 2022.
[22] P. Mishra and S. Lohumi, "Improved Prediction of Protein Content in Wheat Kernels with a Fusion of Scatter Correction Methods in NIR Data Modelling, Biosystems Engineering," vol. 203, pp. 93-97, 2021.
[23] H. Jonsson and J. Gabrielsson, "Comprehensive Chemometrics: 2.11 - Evaluation of Preprocessing Methods," S.D. Brown, R. Tauler, and B. Walczak, Eds.Elsevier, pp. 199-206, 2009.
[24] S. Nuanmeesri, "Mobile Application for the Purpose of Marketing, Product Distribution and Location-Based Logistics for Elderly Farmers,"*Applied Computing and Informatics*, 2020.
[25] S. Nuanmeesri, L. Poomhiran, and K. Ploydanai, "Improving the Prediction of Rotten Fruit Using Convolutional Neural Network," *International Journal of Engineering Trends and Technology*, vol. 69, no. 7, pp. 51-55, 2021.
[26] S. Nuanmeesri, S. Chopvitayakun, P. Kadmateekarun, and L. Poomhiran, "Marigold Flower Disease Prediction Through Deep Neural Network with Multimodal Image," *International Journal of Engineering Trends and Technology*, vol. 69, no. 7, pp. 174-180, 2021.